PULSES IN NONLINEARLY COUPLED SCHRÖDINGER EQUATIONS: II. AN INSTABILITY CRITERION†

RUSSELL K. JACKSON‡ AND CHRISTOPHER K.R.T. JONES§

Abstract. In this work, we derive a geometric criterion for the instability of pulses in a class of nonlinearly coupled Schrödinger equations. Many novel pulses have been observed in such systems both numerically and experimentally, and recent work has provided an understanding of the generation of such pulses. The criterion given here allows an immediate transfer of the information now known about the mechanisms and geometry of pulse creation into a new description of the stability of these same pulses. Additionally, we report the discovery of a secondary bifurcation of (potentially stable) asymmetric pulses that occurs when the value of this criterion changes.

Key words. N-pulses, instability criterion, symmetry breaking, standing waves

AMS subject classifications. 35B35, 35Q55, 70K50

†This work was supported by a grant from the National Science Foundation under award number DMS-0202542.

‡Mathematics Department, US Naval Academy, Annapolis, MD 21402

§Department of Mathematics, University of North Carolina, Chapel Hill, NC 27599

1. Introduction and statement of results. In optical systems, the evolution of an electro-magnetic field is often modeled by a nonlinear Schrödinger (NLS) equation; and when more than one field is present, the model is augmented to include two or more NLS equations, coupled together through the nonlinearity. Solitary waves may serve as information carriers in such systems, and so an understanding of the various waves present, as well as their stability properties, is of paramount importance.

The problem of determining the stability of these waves is often as important as, and perhaps even more interesting than, the problem of existence. If a pulse is not stable, then any noise in the system or a single imperfection in the initial data may cause the pulse to degrade. Stable pulses then correspond to pulses that are physically realizable. In this paper, we introduce a geometric criterion that translates information about the process of pulse construction into information about the presence of positive real eigenvalues for that same pulse. An analysis of this criterion allows us to characterize the stability properties of known pulses, and also to identify new families of (potentially stable) pulses that appear when this criterion changes.

The particular model we consider is the following coupled system:

$$\begin{array}{ccccccccc} \mathrm{i}u_z & + & u_{xx} & + & h_1(|u|^2,|w|^2)u & - & u & = & 0 \\ \mathrm{i}w_z & + & w_{xx} & + & h_2(|u|^2,|w|^2)w & - & rw & = & 0 \end{array} , \tag{1}$$

where $0 < r < 1$ is a normalized propagation constant and $h_1(\cdot)$ and $h_2(\cdot)$ model the material properties. This model appears in various situations: for instance, both Haelterman and Sheppard's model [1] for birefringence in optical fibers, where

$$\begin{array}{rcl} h_1(|u|^2,|w|^2) & = & (1-B)|u|^2 + (1+B)|w|^2 \\ h_2(|u|^2,|w|^2) & = & (1+B)|u|^2 + (1-B)|w|^2 \end{array} , \tag{2}$$

and Ostrovskaya and Kivshar's model [2] for incoherent beam interaction in a biased photorefractive crystal, where

$$h_1(|u|^2,|w|^2) = h_2(|u|^2,|w|^2) = \frac{|u|^2+|w|^2}{1+s(|u|^2+|w|^2)} , \tag{3}$$

can be written in this way. Stationary waves of (1) are real-valued, pulse-like solutions that do not vary with z, and so these waves can be identified as homoclinic orbits in a related finite dimensional ordinary differential equation. For reasonable incarnations of the focusing nonlinearity $h_1(\cdot)$, there are a pair of one-component stationary waves of the form $(U_0(x),0)$ and $(-U_0(x),0)$ that are independent of the parameter r. For particular values of r, the tangent spaces of the global stable and unstable manifolds followed along $(U_0(x),0)$ from $x=+\infty$ and $x=-\infty$, respectively, may coincide; beyond this r value, a number of additional pulses can be found, including a multi-component 1-pulse and also N-pulses for every positive integer N. These pulses have been seen numerically and even experimentally, and recently an analytic description of this bifurcation was given by one of the authors in [3]. This deeper understanding of the process of pulse generation in system (1) allows the opportunity for greater insight into the mechanisms of eigenvalue production in these same pulses.

It has been suggested by Ostrovskaya et al. [4] that the multi-component 1-pulse described above are generally stable for a range of the parameter r beyond the bifurcation value. In particular, as r moves away from the bifurcation value, the corresponding 1-pulse may remain stable even after the total intensity profile

develops a multi-humped structure. We wish to more deeply understand this stability and describe a potential mechanism for the eventual instability as r is increased.

Additionally, in [3], the mechanism for multi-pulse production was shown to vary as the value of r at bifurcation passes through $1/4$. We will also investigate the differences that this variance imposes upon the stability properties of the N-pulses in these two regimes.

To begin, we consider any stationary wave given by $(U(x), W(x))$ for the equation

$$\begin{array}{ccccccccc} \mathrm{i}u_z & + & u_{xx} & + & h_1\left(|u|^2, |w|^2\right) u & - & u & = & 0 \\ \mathrm{i}w_z & + & w_{xx} & + & h_2\left(|u|^2, |w|^2\right) w & - & r\, w & = & 0\,. \end{array}$$

To proceed in the analysis of solutions of these equations, we first decompose the equation above into real and imaginary parts. Letting $u = u_r + \mathrm{i}u_i$ and $w = w_r + \mathrm{i}w_i$, the governing equations may then be rewritten as the real-valued system

$$\begin{array}{ccccccccc} (u_r)_z & + & (u_i)_{xx} & + & h_1\left(u_r^2 + u_i^2, w_r^2 + w_i^2\right) u_i & - & u_i & = & 0 \\ (w_r)_z & + & (w_i)_{xx} & + & h_2\left(u_r^2 + u_i^2, w_r^2 + w_i^2\right) w_i & - & r\, w_i & = & 0 \\ (u_i)_z & - & (u_r)_{xx} & - & h_1\left(u_r^2 + u_i^2, w_r^2 + w_i^2\right) u_r & + & u_r & = & 0 \\ (w_i)_z & - & (w_r)_{xx} & - & h_2\left(u_r^2 + u_i^2, w_r^2 + w_i^2\right) w_r & + & r\, w_r & = & 0\,. \end{array}$$

Since we wish to study the stability of stationary waves in this system, we are interested in the behavior of solutions that are small perturbations of a given stationary wave $(U(x), W(x))$. Since the stationary wave is real-valued, we can then write this as

$$\begin{bmatrix} u_r \\ w_r \\ u_i \\ w_i \end{bmatrix} = \begin{bmatrix} U \\ W \\ 0 \\ 0 \end{bmatrix} + \epsilon \begin{bmatrix} p_1 \\ p_2 \\ q_1 \\ q_2 \end{bmatrix}.$$

We linearize formally by letting $\epsilon \to 0$, and arrive at the linear system

$$\begin{array}{lcr} (p_1)_z + (q_1)_{xx} + h_1(\cdot)\, q_1 & - & q_1 = 0 \\ (p_2)_z + (q_2)_{xx} + h_2(\cdot)\, q_2 & - & r\, q_2 = 0 \\ (q_1)_z - (p_1)_{xx} - h_1(\cdot)\, p_1 - 2U^2 \mathrm{D}_1 h_1(\cdot)\, p_1 - 2UW \mathrm{D}_2 h_1(\cdot)\, p_2 & + & p_1 = 0 \\ (q_2)_z - (p_2)_{xx} - h_2(\cdot)\, p_2 - 2UW \mathrm{D}_1 h_2(\cdot)\, p_1 - 2W^2 \mathrm{D}_2 h_2(\cdot)\, p_2 & + & r\, p_2 = 0\,, \end{array}$$

where the character $\cdot$ replaces U^2, W^2 simply for typographical space considerations. Setting

$$\begin{aligned} L_- &= \tfrac{\mathrm{d}^2}{\mathrm{d}x^2} + \begin{bmatrix} h_1(\cdot) & 0 \\ 0 & h_2(\cdot) \end{bmatrix} + \begin{bmatrix} 1 & 0 \\ 0 & r \end{bmatrix} \\ L_+ &= \tfrac{\mathrm{d}^2}{\mathrm{d}x^2} + \begin{bmatrix} h_1(\cdot) & 0 \\ 0 & h_2(\cdot) \end{bmatrix} + \begin{bmatrix} 2U^2 D_1 h_1(\cdot) & 2UW D_2 h_1(\cdot) \\ 2UW D_1 h_2(\cdot) & 2W^2 D_2 h_2(\cdot) \end{bmatrix} + \begin{bmatrix} 1 & 0 \\ 0 & r \end{bmatrix}, \end{aligned}$$

the linearized equation can be rewritten as

$$\begin{bmatrix} p_1 \\ p_2 \\ q_1 \\ q_2 \end{bmatrix}_z = \begin{bmatrix} 0_{2\times 2} & -L_- \\ L_+ & 0_{2\times 2} \end{bmatrix} \begin{bmatrix} p_1 \\ p_2 \\ q_1 \\ q_2 \end{bmatrix}.$$

Writing $v(x,z) = (p_1, p_2, q_1, q_2)$, we study instability by searching for solutions of this equation of the form $v(x,z) = v(x)\mathrm{e}^{\lambda z}$ where $v(x)$ is a bounded function with decaying tails and λ is a complex scalar. Of interest then are the eigenvalue equations

$$\begin{aligned} L_- \begin{bmatrix} q_1 \\ q_2 \end{bmatrix} &= -\lambda \begin{bmatrix} p_1 \\ p_2 \end{bmatrix} \\ L_+ \begin{bmatrix} p_1 \\ p_2 \end{bmatrix} &= \lambda \begin{bmatrix} q_1 \\ q_2 \end{bmatrix} . \end{aligned}$$

Explicitly, this is the system

$$\begin{array}{rcrcrcr} (p_1)_{xx} & = & \lambda q_1 & - & h_1(\cdot)p_1 - 2U^2\mathrm{D}_1 h_1(\cdot)p_1 - 2UW\mathrm{D}_2 h_1(\cdot)p_2 & + & p_1 \\ (p_2)_{xx} & = & \lambda q_2 & - & h_2(\cdot)p_2 - 2UW\mathrm{D}_1 h_2(\cdot)p_1 - 2W^2\mathrm{D}_2 h_2(\cdot)p_2 & + & r\ p_2 \\ (q_1)_{xx} & = & -\lambda p_1 & - & h_1(\cdot)q_1 & + & q_1 \\ (q_2)_{xx} & = & -\lambda p_2 & - & h_2(\cdot)q_2 & + & r\ q_2. \end{array}$$

Letting $(v_1, v_2, v_3, v_4) = (p_1, p_2, q_1, q_2)$ and introducing the variables $v_5, \ldots, v_8$ as the derivatives with respect to x of $v_1, \ldots, v_4$, respectively, we can write this as an eight dimensional system of first order equations

$$v' = \left[\begin{array}{c|c} 0_{4\times 4} & I_{4\times 4} \\ \hline \Lambda_{4\times 4} & 0_{4\times 4} \end{array} \right] v \tag{4}$$

where $\Lambda_{4\times 4}$ is given by

$$\left[\begin{array}{cc|cc} 1 - h_1(\cdot) - 2U^2\mathrm{D}_1 h_1(\cdot) & -2UW\mathrm{D}_2 h_1(\cdot) & \lambda & 0 \\ -2UW\mathrm{D}_1 h_2(\cdot) & r^2 - h_2(\cdot) - 2W^2\mathrm{D}_2 h_2(\cdot) & 0 & \lambda \\ \hline -\lambda & 0 & 1 - h_1(\cdot) & 0 \\ 0 & -\lambda & 0 & r - h_2(\cdot) \end{array} \right] . \tag{5}$$

This formulation emphasizes the differing dependence on the real and imaginary parts of the solutions. It is this formulation that we will exploit in order to write down, and then analyze, the geometric instability criterion in Section 3.

Before doing so, however, it is sometimes convenient to rearrange the variables in order to better visualize the distinct roles of the two pulse components. To this end, by reordering the components of the vector v, the matrix $\Lambda_{4\times 4}$ may alternatively be written as

$$\left[\begin{array}{cc|cc} 1 - h_1(\cdot) - 2U^2\mathrm{D}_1 h_1(\cdot) & \lambda & -2UW\mathrm{D}_2 h_1(\cdot) & 0 \\ -\lambda & 1 - h_1(\cdot) & 0 & 0 \\ \hline -2UW\mathrm{D}_1 h_2(\cdot) & 0 & r - h_2(\cdot) - 2W^2\mathrm{D}_2 h_2(\cdot) & \lambda \\ 0 & 0 & -\lambda & r - h_2(\cdot) \end{array} \right] . \tag{6}$$

When one of the pulse components is zero, the cross terms disappear and this system is easily seen to decouple into a pair of four dimensional systems. This formulation allows us to easily understand the spectrum of the one-component pulse $(U_0(x), 0)$ and, by continuation, the absence of positive real eigenvalues of the multi-component 1-pulse nearby the bifurcation value.

For either formulation, if there is a bounded solution $v(x)$ of this system associated with an eigenvalue λ with $\mathrm{Re}(\lambda) > 0$, then $v(x)e^{\lambda z}$ is an unstable mode of the linearized equation. Moreover, this eigenvalue problem has a four-fold symmetry; *i.e.*, if λ is an eigenvalue of this system, then so are $\bar{\lambda}$, $-\lambda$, and $-\bar{\lambda}$, where $^-$ denotes

complex conjugation. Hence, the only chance a pulse has to be stable is for its entire spectrum to be confined to the imaginary axis.

In Section 2, we use the formulation of the eigenvalue equation given by (6) in order to describe the spectrum of the single-component pulse $(U_0(x), 0)$ and the multi-component 1-pulses nearby the bifurcation values. We can completely characterize the spectrum of the one-component pulse, and a characterization of the spectrum of the bifurcating multi-component pulses quickly follows (at least nearby the bifurcation point). In particular, for the nonlinearities $h_1(\cdot)$ given above, there are no real non-zero eigenvalues and the pulses may be stable.

In Section 3, we derive a geometric instability criterion that provides information about the presence of positive real eigenvalues, in relation to the formulation given by (5). Using the geometric information given in the bifurcation analysis in [3], we can begin a characterization of the stability of all of the pulses seen in that paper. In particular, an analysis of this criterion supports the assertions of the previous section. Moreover, this citerion shows that N-pulses in the regime where the bifurcation parameter $r \geq 1/4$ are all inherently unstable. Startlingly, when the bifurcation parameter r is smaller than $1/4$, the resulting N-pulses do not necessarily have any real positive eigenvalues!

Finally, as the multi-component pulses are continued away from the original bifurcation, the instability criterion may change, marking the presence of a real positive eigenvalue. At the onset of this change, a pair of asymmetric pulses bifurcate from the original multi-component pulse. In many different models, see Jones [8] or Jackson and Weinstein [16] for example, it is the case that beyond such a bifurcation, the symmetric wave is unstable and the asymmetric waves are stable. In this case also, the instability criterion provides the possibility of stability for these bifurcating asymmetric waves.

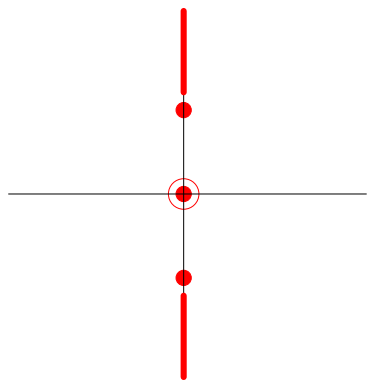

FIG. 1. *The spectrum of the first subsystem (7).*

2. Elementary results concerning the spectrum. We are now prepared to begin our search for eigenvalues for pulses in the coupled nonlinear Schrödinger equations. For the stationary wave $(U_0(x), 0)$ with trivial w-component, the eigenvalue equation (4) decouples into a pair of 4×4 systems

$$\begin{bmatrix} v_1 \\ v_2 \\ v_5 \\ v_6 \end{bmatrix}' = \left[\begin{array}{cc|cc} 0 & 0 & 1 & 0 \\ 0 & 0 & 0 & 1 \\ \hline 1 - h_1(\cdot) - 2U^2 \mathrm{D}_1 h_1(\cdot) & \lambda & 0 & 0 \\ -\lambda & 1 - h_1(\cdot) & 0 & 0 \end{array}\right] \begin{bmatrix} v_1 \\ v_2 \\ v_5 \\ v_6 \end{bmatrix} \tag{7}$$

and

$$\begin{bmatrix} v_3 \\ v_4 \\ v_7 \\ v_8 \end{bmatrix}' = \left[\begin{array}{cc|cc} 0 & 0 & 1 & 0 \\ 0 & 0 & 0 & 1 \\ \hline r - h_2(\cdot) & \lambda & 0 & 0 \\ -\lambda & r - h_2(\cdot) & 0 & 0 \end{array}\right] \begin{bmatrix} v_3 \\ v_4 \\ v_7 \\ v_8 \end{bmatrix}. \tag{8}$$

The spectrum of the stationary wave will then be the union of the spectra of these two individual systems. These two contributions to the spectrum are described in the following two lemmas.

LEMMA 1. *For the first subsystem (7), the essential spectrum is purely imaginary encompassing the entire imaginary axis except for an open gap between* $-\mathrm{i}$ *and* i*, in particular,* $\sigma_e = \{x + \mathrm{i}y \mid x = 0, |y| \geq 1\}$*. There is an eigenvalue at the origin which has geometric multiplicity* 2 *and algebraic multiplicity* 4*. For the saturable nonlinearity of the Ostrovskaya–Kivshar problem, there are also a pair of eigenvalues in the gap on the imaginary axis near the branch points of the essential spectrum. See Figure 1.*

Proof. The first system (7) is the usual Schrödinger equation with an intensity–dependent nonlinearity and the spectrum is well known. The essential spectrum is defined à la Henry [5], and contains the set of points at which the asymptotic matrix has eigenvalues on the imaginary axis. It is a quick calculation that the asymptotic matrix has eigenvalues $\pm\sqrt{1 \pm \mathrm{i}\lambda}$ and hence λ is in the essential spectrum if and only if either $1 + \mathrm{i}\lambda$ or $1 - \mathrm{i}\lambda$ is a non-positive real number. The point spectrum at zero is determined by the symmetries present in the system. There is an eigenfunction

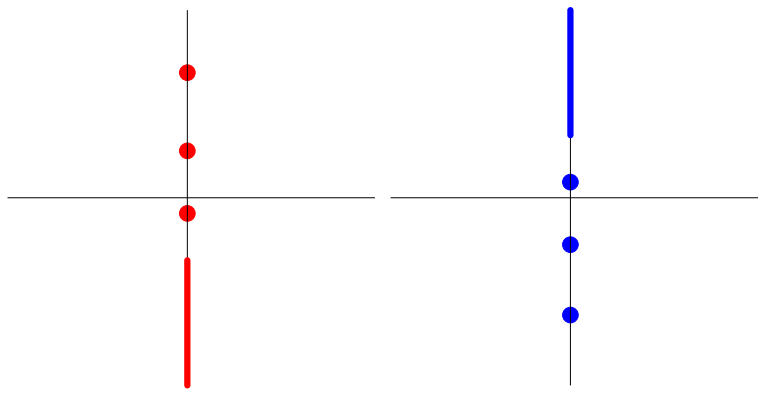

FIG. 2. *The spectrum of the second subsystem (8) is the union of two reflected components.*

$(U'(x), 0, U''(x), 0)$ associated with the translation invariance of the solution; *i.e.*, if $U(x)$ is a solution then so is $U(x+\epsilon)$ for any ϵ. Similarly, there is an eigenfunction $(0, U(x), 0, U'(x))$ stemming from the phase invariance; given a solution $U(x)$, $U(x)\mathrm{e}^{\mathrm{i}\epsilon}$ is also a solution for any ϵ.

Depending upon the specific form of the function $h_1(\cdot)$ there may be other point spectrum as well. For instance, with the saturable nonlinearity used by Ostrovskaya and Kivshar (3), with saturability parameter s, there will be a pair of eigenvalues in the gap, one at a distance $O(s^2)$ from each branch point, see Kapitula and Sandstede [6]. □

LEMMA 2. *For the second subsystem (8), the essential spectrum is purely imaginary encompassing the entire imaginary axis except for an open gap between* $-\mathrm{i}r$ *and* $\mathrm{i}r$*, in particular,* $\sigma_e = \{x+\mathrm{i}y \mid x = 0, |y| \geq r\}$*. There are also a finite number of eigenvalues on the imaginary axis, whose distance from one branch point or the other are independent of* r*. Particularly, there is a positive descending sequence* $r_0, r_1, \ldots, r_k$ *such that* $\mathrm{i}(r - r_j)$ *and* $-\mathrm{i}(r - r_j)$ *are eigenvalues, for* $0 \leq j \leq k$*. Depending upon the parameter* r*, these values may appear either in the gap or embedded within the essential spectrum. See Figure 2.*

Proof. To more readily visualize the spectrum associated with the second system (8), we make the substitutions $\tilde{\lambda} = -\mathrm{i}\lambda$ and $\tilde{v_4} = -\mathrm{i}v_4$. This yields the system

$$\begin{array}{rcrcr} v_3'' & = & r - h_2(\cdot)\, v_3 & - & \tilde{\lambda}\, \tilde{v}_4 \\ \tilde{v_4}'' & = & -\tilde{\lambda}\, v_3 & + & r - h_2(\cdot)\, \tilde{v}_4. \end{array}$$

We then consider eigenfunctions with the special form $\tilde{v}_4 = v_3$, and find the Sturm–Liouville problem

$$v_3'' \quad = \quad (r - \tilde{\lambda})\, v_3 - h_2(\cdot)\, v_3.$$

Letting $\tilde{r} = r - \tilde{\lambda}$, we arrive at the same equation that was used in the existence study to identify the points of degeneracy (the bifurcation values) of this same pulse. In particular, it is a Sturm-Liouville problem and has a finite number of eigenvalues $\tilde{r}_0, \tilde{r}_1, \ldots, \tilde{r}_k$ corresponding to eigenfunctions with, respectively, $0, 1, \ldots, k$ zeros. Returning to the original variables, the second subsystem has essential spectrum $\sigma_e = \{x + \mathrm{i}y \mid x = 0, y \geq r\}$ and eigenvalues given by $\mathrm{i}(r - \tilde{r}_0), \mathrm{i}(r - \tilde{r}_1), \ldots, \mathrm{i}(r - \tilde{r}_k)$.

Similarly, if we look for eigenfunctions of the form $\tilde{v}_4 = -v_3$, we find the problem

$$v_3'' \quad = \quad (r + \tilde{\lambda})\, v_3 - h_2(\cdot)\, v_3.$$

This provides the other component of the essential spectrum $\sigma_e = \{x + \mathrm{i}y \mid x = 0, y \leq -r\}$ and eigenvalues given by $-\mathrm{i}(r - \tilde{r}_0), -\mathrm{i}(r - \tilde{r}_1), \ldots, -\mathrm{i}(r - \tilde{r}_k)$.

The full spectrum of the second subsystem is made up of these two reflected pieces. □

It is clear from the analysis above that the degeneracy of the single-component pulse $U_0(x)$ when $r = r_0, r_1, \ldots, r_k$, the values that mark the onset of a multi-component bifurcating pulse, correspond to a conjugate pair of eigenvalues meeting at zero in the eigenvalue problem for that pulse. If we continue to follow the one-component pulse $U_0(x)$ through one of these values of the parameter r, these conjugate eigenvalues pull rigidly through each other and continue along the imaginary axis – indicating that the pulse $U_0(x)$ is stable for all r. However, accounting for these near zero eigenvalues as we follow the symmetric bifurcating multi-component pulses is critical in determining the stability properties of these pulses in a neighborhood of the bifurcation at $r = r_i$. The next lemma specifies the fate of the two conjugate eigenvalues as we follow the bifurcating multi–component pulse.

LEMMA 3. *For $r \geq r_i$, the bifurcating multi-component pulse has a zero eigenvalue of geometric multiplicity* 3 *and algebraic multiplicity* 6.

Proof. Recall that the single-component pulse generally, *i.e.*, away from the bifurcation points, has an eigenvalue at the origin with geometric multiplicity 2 and algebraic multiplicity 4. This corresponds to the translation and phase invariances. However, because of the form of the nonlinearity, the bifurcating multi-component pulse has a phase invariance associated with *each* nontrivial pulse component. Therefore, the two new eigenvalues are locked at zero in order to account for the nontrivial phase invariance of the (now nonzero) w-component of the bifurcating pulse. □

This provides the somewhat surprising result that, near the bifurcation value $r = r_i$, *both* the single-component pulse $U_0(x)$ and the bifurcating multi-component 1-pulse may be stable, as the near zero eigenvalues at $r = r_i$ move along the imaginary axis in one case and are locked at zero in the other. In neither case do they move onto the real axis, away from zero.

REMARK 1. *Although there are no real positive eigenvalues for the bifurcating pulse, we have not ruled out the possibility of other unstable eigenvalues (with nonzero imaginary part) emerging. As desribed above, no eigenvalues with positive real part appear due to the convergence of eigenvalues at the origin that spurs the bifurcation. Additionally, any isolated eigenvalues of algebraic multiplicity one in the gap along the imaginary axis cannot leave this axis because of the four-fold symmetry of the spectrum in this problem. However, the eigenvalues embedded within the essential spectrum* may *leave the imaginary axis regardless of their multiplicity. This possibility has been studied carefully by Pelinovsky and Yang [7].*

3. An instability criterion and its implications. In this section, we derive an instability criterion for the stationary pulse solutions of (1) and describe its implications for the stability of the many known solutions.

Recall that the eigenvalue equation can be written as

$$\begin{bmatrix} 0_{2\times 2} & -L_- \\ L_+ & 0_{2\times 2} \end{bmatrix} \begin{bmatrix} p_1 \\ p_2 \\ q_1 \\ q_2 \end{bmatrix} = \lambda \begin{bmatrix} p_1 \\ p_2 \\ q_1 \\ q_2 \end{bmatrix}$$

where

$$\begin{aligned} L_- &= \tfrac{\mathrm{d}^2}{\mathrm{d}x^2} + \begin{bmatrix} h_1(\cdot) & 0 \\ 0 & h_2(\cdot) \end{bmatrix} + \begin{bmatrix} 1 & 0 \\ 0 & r \end{bmatrix} \\ L_+ &= \tfrac{\mathrm{d}^2}{\mathrm{d}x^2} + \begin{bmatrix} h_1(\cdot) & 0 \\ 0 & h_2(\cdot) \end{bmatrix} + \begin{bmatrix} 2U^2 D_1 h_1(\cdot) & 2UWD_2 h_1(\cdot) \\ 2UWD_1 h_2(\cdot) & 2W^2 D_2 h_2(\cdot) \end{bmatrix} + \begin{bmatrix} 1 & 0 \\ 0 & r \end{bmatrix}. \end{aligned}$$

Both Grillakis [9] and Jones [8] provide a criterion relating the spectrum of the operators L_+ and L_- with the spectrum of the operator

$$N = \begin{bmatrix} 0_{2\times 2} & -L_- \\ L_+ & 0_{2\times 2} \end{bmatrix}.$$

The operators L_+ and L_- are both self–adjoint and hence the spectrum of each will be contained entirely within the real axis. However, it is not immediately clear how the spectrum of the operator N relates to the spectra of L_+ and L_-. In particular, the spectrum of N will not typically be real; as we have seen already, much of it will lie upon the imaginary axis. We define

$$\begin{aligned} n(L_+) &= \text{the number of positive eigenvalues of } L_+ \\ n(L_-) &= \text{the number of positive eigenvalues of } L_- \\ z(L_-) &= \text{the number of zero eigenvalues of } L_- \end{aligned}$$

where the eigenvalues are counted including multiplicity. In the case that L_+ and L_- are scalar operators, Jones [8] provides an instability criterion, namely, that if $n(L_+) - n(L_-) \neq 0, 1$, then N has a real positive eigenvalue. The proof is geometric in nature, and involves a shooting argument in the space of Lagrangian planes $\Lambda(2)$. For higher dimensional systems, Grillakis [9] provides a generalized criterion using a functional analytic approach. In particular, if we write

$$Y = [\ker(L_+) \cup \ker(L_-)]^{\perp}$$

and let

$$\begin{aligned} \hat{L}_+ &= \text{the restriction of } L_+ \text{ to } Y \\ \hat{L}_-^{-1} &= \text{the restriction of } L_-^{-1} \text{ to } Y \end{aligned}$$

then Grillakis' theorem states that there are exactly

$$\max\{n(\hat{L}_+), n(\hat{L}_-^{-1})\} - \dim(C(\hat{L}_+) \cap C(\hat{L}_-^{-1}))$$

positive real eigenvalues. Here, $C(L) = \{y \in Y \mid \langle Ly, y\rangle < 0\}$ denotes the negative cone of an operator L. We use Grillakis' theorem to derive a generalization of Jones' criterion suitable for our purposes. This derivation parallels the work of Yew [10].

LEMMA 4. *If $n(L_+) - z(L_-) - n(L_-) > 0$, then N has a real positive eigenvalue.*

Proof. To prove this criterion, we must bound the quantities present in Grillakis' theorem. In particular, to estimate the quantities $n(\hat{L}_+)$ and $n(\hat{L}_-^{-1})$ we must consider how projection onto the subspace Y affects the indices. Because L_+ is self–adjoint, the negative eigenspace of L_+ is orthogonal to its kernel $\ker(L_+)$, and hence is influenced only by projection off of $\ker(L_-)$. At worst, projection off of $\ker(L_-)$ reduces the dimension of the negative eigenspace of L_+ by $\dim(\ker(L_-)) = z(L_-)$ and hence

$$\begin{aligned} \max\{n(\hat{L}_+), n(\hat{L}_-^{-1})\} &= n(\hat{L}_+) \\ &\geq n(L_+) - z(L_-) \ . \end{aligned}$$

Likewise, at best, projection off of $\ker(L_+)$ leaves the dimension of the negative eigenspace of L_- unchanged. Therefore

$$\begin{aligned} \dim(C(\hat{L}_+) \cap C(\hat{L}_-^{-1})) &\leq \min\{\dim(C(\hat{L}_+)), \dim(C(\hat{L}_-^{-1}))\} \\ &\leq \min\{n(\hat{L}_+), n(\hat{L}_-^{-1})\} \\ &= n(\hat{L}_-^{-1}) \\ &\leq n(L_-) \end{aligned}$$

and it follows that

$$\max\{n(\hat{L}_+), n(\hat{L}_-^{-1})\} - \dim(C(\hat{L}_+) \cap C(\hat{L}_-^{-1})) \geq n(L_+) - z(L_-) - n(L_-) \ .$$

Applying the theorem of Grillakis, the lemma follows immediately. □

This lemma provides a useful criterion for the instability of a pulse, but does not imply stability in the case that $n(L_+) - z(L_-) - n(L_-) \leq 0$. However, each of the components of this criterion can be read off quickly for the known stationary waves and hence can provide immediate information concerning the stability of stationary pulses. Additionally, a change in the value of this criterion along the continuation of a pulse indicates not only the possible onset of instability, but also a degeneracy of the pulse, and therefore a further bifurcation of stationary waves.

We will use the condition given in Lemma 4 to examine the (in)stability properties of the stationary solutions of (1).

3.1. The one-component pulse, revisited. As an exercise, we can check the criterion given in Lemma 4 for the single component pulse $(U_0(x), 0)$ considered in the previous section. For this pulse, both of the operators L^+ and L^- decouple further. L^+ is given by

$$L_+ = \frac{\mathrm{d}^2}{\mathrm{d}x^2} + \begin{bmatrix} h_1(\cdot) & 0 \\ 0 & h_2(\cdot) \end{bmatrix} + \begin{bmatrix} 2U^2 D_1 h_1(\cdot) & 0 \\ 0 & 0 \end{bmatrix} - \begin{bmatrix} 1 & 0 \\ 0 & r \end{bmatrix} .$$

Hence L_+ can be broken into scalar operators with spectrum that can be determined by a Sturm-Liouville argument. The first operator

$$L_+^{(1)} = \frac{\mathrm{d}^2}{\mathrm{d}x^2} + h_1(\cdot) + 2U^2 \mathrm{D}_1 h_1(\cdot) - 1$$

has a zero eigenvalue reflecting the translation invariance of the single component pulse. Moreover, since the eigenfunction $U'(x)$ has one zero, there is exactly one positive eigenvalue of this operator. The second operator

$$L_+^{(2)} = \frac{\mathrm{d}^2}{\mathrm{d}x^2} + h_2(\cdot) - r$$

has a non-negative number $j(r)$ of positive eigenvalues depending upon the value of r. In particular, if $r_{i+1} \leq r < r_i$, then $j(r) = i$. So $n(L_+^{(2)}) = j(r)$.

The operator L_- is given by

$$L_- = \frac{\mathrm{d}^2}{\mathrm{d}x^2} + \begin{bmatrix} h_1(\cdot) & 0 \\ 0 & h_2(\cdot) \end{bmatrix} - \begin{bmatrix} 1 & 0 \\ 0 & r \end{bmatrix}$$

and can also be broken into two scalar operators. The first,

$$L_-^{(1)} = \frac{\mathrm{d}^2}{\mathrm{d}x^2} + h_1(\cdot) - 1 \ ,$$

has a zero eigenvalue associated with the phase invariance of the wave and hence $z(L_-^1) = 1$. Since the eigenfunction $U(x)$ has no zeros, there are no positive eigenvalues of this operator, *i.e.*, $n(L_-^{(1)}) = 0$. The second operator,

$$L_-^{(2)} = \frac{\mathrm{d}^2}{\mathrm{d}x^2} + h_2(\cdot) - r \ ,$$

is the same as $L_+^{(2)}$ in this case and has the same non-negative number $j(r)$ of positive eigenvalues. $L_-^{(2)}$ has a zero eigenvalue only when the pulse solution $U_0(x)$ is degenerate, so $z(L_-^{(2)}) = 1$ if $r \in \{r_0, r_1, \ldots, r_k\}$ and $z(L_-^{(2)}) = 0$ otherwise.

So, $n(L_+) = 1 + j(r)$, $z(L_-) = 1$ or 2 and $n(L_-) = j(r)$. Hence $n(L_+) - z(L_-) - n(L_-) = -1$ or 0. Therefore, we do not *a priori* expect an instability in this stationary wave. This is, of course, a good sign, as we proved this wave to be stable in the previous section.

3.2. The computation of $n(L_+)$ using the Maslov Index. For any stationary pulse in this system, the values $n(L_-)$ and $z(L_-)$ are easy to compute. As in the case for the single-component pulse $U_0(x)$ above, the operator L_- decouples as

$$L_- = \frac{\mathrm{d}^2}{\mathrm{d}x^2} + \begin{bmatrix} h_1(\cdot) & 0 \\ 0 & h_2(\cdot) \end{bmatrix} - \begin{bmatrix} 1 & 0 \\ 0 & r \end{bmatrix} .$$

For a pulse with two non-trivial components, the two resulting scalar operators each have a zero eigenvalue associated with the phase invariance of the two individual components of the solution, hence $z(L_-) = 2$. The value of $n(L_-)$ is then determined by the number of zeros of the two pulse components themselves. The successful application of the instability criterion then depends upon the more complicated calculation of $n(L_+)$.

The key to the calculation of $n(L_+)$ for any pulse is the notion of winding. In the case above, L_+ decoupled into a pair of scalar evolution equations, where the flow could be interpretted as occuring on two circles $S^1 \times S^1$. The circle has fundamental group $\mathbb{Z}$, and so the winding number is straightforward to define and is equivalent to the number of nodes of the zero-eigenfunction.

Unfortunately, for multi-component pulses, L_+ does not decouple in this way and the flow is naturally interpretted as occuring on the Grassmannian space $G^2(\mathbb{R}^4)$, *i.e.*, the set of two-dimensional subspaces within $\mathbb{R}^4$. This space has fundamental group $\mathbb{Z}_2$ and so a notion of winding is not immediately available. Fortunately, because of the Hamiltonian structure of (2) and (3), solutions of L_+ also preserve Lagrangain

planes, and so can be tracked in the Lagrangian subspace $\Lambda(2)$ of $G^2(\mathbb{R}^4)$; and $\Lambda(2)$ has fundamental group $\mathbb{Z}$.

For calculations in these spaces, we make use of the exterior power space $\Lambda^2(\mathbb{R}^4)$. This space is six dimensional and we can explicitly derive the system in $\Lambda^2(\mathbb{R}^4)$ induced by the eigenvalue problem for L_+ given in (5):

$$
\begin{array}{rcl}
P_{12}' & = & P_{14} - P_{23} \\
P_{13}' & = & -f_c(\cdot)P_{12} \\
P_{24}' & = & f_c(\cdot)P_{12} \\
P_{14}' & = & P_{34} + ((r+\lambda) - f_w(\cdot))P_{12} \\
P_{23}' & = & -P_{34} - ((1+\lambda) - f_u(\cdot))P_{12} \\
P_{34}' & = & ((1+\lambda) - f_u(\cdot))P_{14} - ((r+\lambda) - f_w(\cdot))P_{23} + f_c(\cdot)\,(P_{13} - P_{24})\,,
\end{array}
\tag{9}
$$

where f_u, f_w and f_c have been introduced in place of $h_1(\cdot) + 2U^2\mathrm{D}_1 h_1(\cdot)$, $h_2(\cdot) + 2W^2\mathrm{D}_2 h_2(\cdot)$ and $2UW\mathrm{D}_1 h_2(\cdot)$, respectively, for the sake of brevity. Not every set of coefficients P_{ij} corresponds to a point in $G_2(\mathbb{R}^4)$. The set of numbers P_{ij} are the Plücker coordinates if the following *Grassmannian condition* is satisfied:

$$P_{12}P_{34} - P_{13}P_{24} + P_{14}P_{23} = 0\ . \tag{10}$$

A quick calculation indeed shows that

$$(P_{12}P_{34} - P_{13}P_{24} + P_{14}P_{23})' = 0\ .$$

Additionally, because (1) is Hamiltonian, (9) also preserves Lagrangian planes, $\Lambda(2)$. This invariance is given by the following *Lagrangian condition*:

$$P_{13} + P_{24} = 0\ . \tag{11}$$

An even quicker calculation shows that

$$(P_{13} + P_{24})' = 0$$

and hence both the Lagrangian and the Grassmannian conditions will continue to be satisfied as x evolves, if only the initial conditions satisfy them.

We can therefore use *the Maslov index* to count the number of real positive eigenvalues of L_+. Because $\Lambda(2)$ is a 3–dimensional manifold, a concrete visualization of this space and the winding within it can be given. In particular, $\Lambda(2)$ can be seen as $S^2 \times [-1, +1]$ where the spheres at $+1$ and -1 are identified via the antipodal map (see Jones [8]). Specifically, $\Lambda(2)$ is a fiber bundle over S^1 with fiber S^2 and clutching function the antipodal map. The fundamental group is $\mathbb{Z}$ and the projection onto S^1 gives the winding — this winding is the Maslov index. In order to exploit this winding, it is natural to use the covering space of $\Lambda(2)$ — this covering space is $S^2 \times \mathbb{R}$ and will be denoted $C(2)$.

The eigenvalue problem for L_+ can then be reformulated as a shooting problem in $\Lambda(2)$. Before detailing this shooting problem, we require the notion of the train of a point $\psi \in \Lambda^2$. We define the *train of* ψ, denoted $D(\psi)$ to be the set of all $\phi \in \Lambda(2)$ that have a nontrivial intersection with ψ, where ψ and ϕ are considered as two-dimensional subspaces of $\mathbb{R}^4$. For any $\phi \in \Lambda(2)$, the train $D(\psi)$ can be lifted to $\hat{D}(\psi)$ in the covering space $C(2)$. In $C(2)$, $\hat{D}(\psi)$ has the appearance of the union of infinitely many cones, joined base to base and vertex to vertex. Each vertical slice is

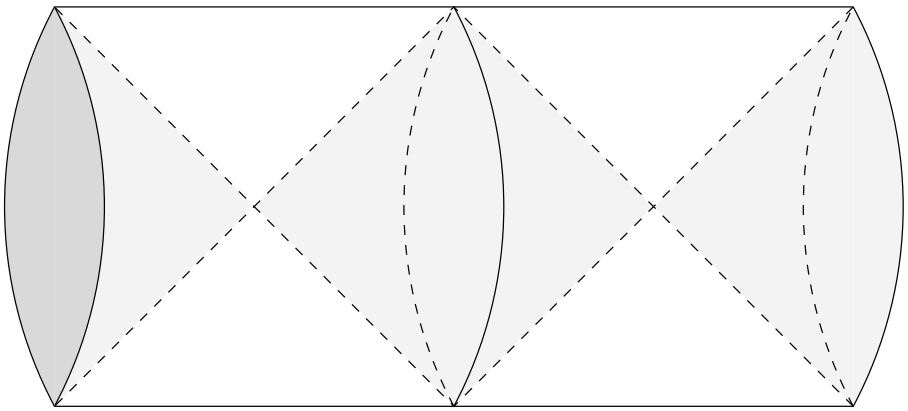

FIG. 3. *The covering space $C(2)$ for the space of Lagrangian planes $\Lambda(2)$.*

a disk and the fiber S^2 is obtained by identifying the boundary of this disk to a single point. $\hat{D}(\psi)$ partitions $C(2)$ into an infinite number of components, see Figure 3.

For a fixed train $\hat{D}(\beta)$, any curve in $\Lambda(2)$ starting at a point α and ending at a point β' can then be lifted to $C(2)$. We can then define the *Maslov index* of a path starting at a point α and ending at β', for $\alpha \notin \hat{D}(\beta)$ as either: the index of intersection of this path with $\hat{D}(\beta)$ if $\beta \neq \beta'$, or $1 +$ the index of intersection of this path with $\hat{D}(\beta)$ if $\beta = \beta'$. We are required to distinguish between paths ending at the vertex β and paths ending at other points because the intersection of a path with the vertex is two dimensional, whereas intersections with other parts of the train are one dimensional.

The shooting argument is then clear. For a fixed $\lambda \in \mathbb{R}$, we can identify the two points $W_-^u \in \Lambda(2)$ associated with the unstable subspace of the asymptotic system and $W_+^s \in \Lambda(2)$ which is associated with the stable subspace. Lifting W_-^u to a point $\hat{W}_-^u$ in the covering space, λ is an eigenvalue if and only if there is a connecting orbit between $\hat{W}_-^u$ and $\hat{D}(W_+^s)$.

Letting $I(\lambda)$ denote the Maslov index of the path in $C(2)$ with α-limit set $\hat{W}_-^u$ for a particular λ, we have the following lemmas.

LEMMA 5. *If $\lambda_1 < \lambda_2$, then the number of eigenvalues $\lambda \in [\lambda_1, \lambda_2)$ equals $I(\lambda_1) - I(\lambda_2)$.*

LEMMA 6. *The number of eigenvalues $\lambda \in [\lambda_1, \infty)$ equals $I(\lambda_1)$.*

The fact that $I(\lambda_1) - I(\lambda_2)$ provides a lower bound for the number of eigenvalues is clear. Equality requires a monotonicity argument – we defer to Deng [11] in this matter. The second lemma is a result of the loss of ellipticity of the transient system for λ large.

The Maslov index $I(\lambda)$ is related to the horizontal distance traveled by a path in $C(2)$ projected onto $\mathbb{R}$ (the covering space of the fiber bundle S^1). However, some information is lost in this projection, as two points in the same fiber may be in separate components of $C(2)$ (they may lie on opposite sides of the train) and the Maslov index of paths ending at these two points will differ by 1. However, because the equation for L_+ reduces to the equation of variations when $\lambda = 0$, we know *a priori* that $\lambda = 0$ is an eigenvalue (this eigenvalue is associated with the translation invariance of the

stationary wave). Therefore, the orbit with α-limit $\hat{W}^u_-$ connects exactly with the train $\hat{D}(W^s_+)$. In particular, we can compute the Maslov index $I(0)$ exactly using only the angular information associated with the aforementioned projection onto $\mathbb{R}$. And $n(L_+) = I(0) - 1$.

The space of Lagrangian planes $\Lambda(2)$ can be represented as a homogeneous space: $\Lambda(2) \cong U(2)/O(2)$, where $U(2)$ is the group of unitary matrices and $O(2)$ is the subgroup of real orthogonal matrices (see Arnol'd [14]). With this view, the desired projection onto S^1 is achieved via the map $\mathrm{Det}^2(\cdot)$. The angular equation associated with the map $\mathrm{Det}^2(\cdot)$ is then

$$\kappa = \tan^{-1} \frac{\mathrm{Im}\,\mathrm{Det}^2(\cdot)}{\mathrm{Re}\,\mathrm{Det}^2(\cdot)} \ .$$

In Bose and Jones [15], this formulation is used to derive formulae for κ and κ' in Plücker coordinates:

$$\kappa = \tan^{-1} \frac{2(P_{14} - P_{23})(P_{12} - P_{34})}{(P_{14} - P_{23})^2 - (P_{12} - P_{34})^2}$$

and

$$\kappa' = \frac{2(P'_{12} - P'_{34})(P_{14} - P_{23}) - (P'_{14} - P'_{23})(P_{12} - P_{34})}{(P_{14} - P_{23})^2 + (P_{12} - P_{34})^2} \ .$$

We can use these expressions for κ in order to quickly evaluate $I(\lambda)$, and therefore $n(L_+)$, numerically for any stationary wave.

Moreover, for the bifurcating stationary waves (multi-component 1-pulses and N-pulses) given by Jackson [3], we can determine $I(\lambda)$ analytically. Near the bifurcation value, this work demonstrates how the global unstable manifold, W^u, intersects transverse sections Σ_{out} and Σ_{in} defined near the origin on successive excursions near the one-component pulse $(U_0(x), 0)$ and its reflection $(-U_0(x), 0)$. In particular, we can pick out points in these sections associated with the passage of each stationary pulse. The evolution of the orbit with α-limit set $\hat{W}^u_-$ can then be uniquely identified since it must be spanned by 1) a vector transverse to the section in the direction of the flow and 2) a vector tangent to the global unstable manifold W^u within the section. Using this infomation, we can compute the total winding $I(0)$ of the orbit with α-limit set $\hat{W}^u_-$ throughout its evolution. This will be pursued for the multi-component 1-pulse and the N-pulses in the following subsections.

3.3. The multi-component 1-pulse, revisited. As the parameter r increases through a bifurcation value $r = r_i$, the one-component pulse $U_0(x)$ passes through a degeneracy. The orbit in $C(2)$ with α-limit $\hat{W}^u_-$ terminates at the vertex of the train for this value of r. Because L_+ decouples into two smaller systems in this case, and winding along $U_0(x)$ in S^1 is monotonically decreasing in r, we easily calculate that the Maslov Index $I(0)$ drops from $i+2$ to $i+1$ at this same point for the one-component pulse, as in the previous section. However, note from Figure 4 that the multi-component pulse bifurcating from $U_0(x)$ as r passes through r_i does not observe this relaxing of the winding and, along this pulse, the tangent space of the global unstable manifold rotates π radians farther than it does for the single-component pulse. Therefore $I(0) = i + 2$ in this case and so

$$n(L+) - z(L_-) - n(L_-) = (i+2) - (2) - (i) = 0 \ .$$

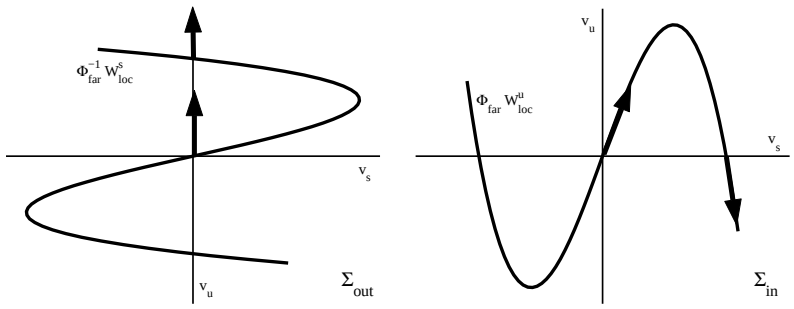

FIG. 4. *A view of the winding from the bifurcation picture for the* 1*-pulses. The orbit in* $C(2)$ *with* α*-limit* $\hat{W}_{-}^{u}$ *rotates farther for the bifurcating multi-component* 1*-pulse than it does for the continuation of the one-component pulse.*

In particular, this pulse may be stable.

Note that if, as we continue the multi-component 1-pulse farther from the bifurcation point, this pulse itself becomes degenerate, the associated orbit with α-limit set $\hat{W}_{-}^{u}$ in $C(2)$ will again intersect the vertex of the train. On opposite sides of the degeneracy, then, we expect this orbit to have different values of the Maslov index $I(0)$ and hence different values for $n(L_+)$. Whereas, pulses bifurcating from the single-component pulse $U_0(x)$ when it became degenerate had a shot a stability, since the change in the Maslov Index was offset by a corresponding change in $z(L_-)$, bifurcations from pulses with two non-trivial components do not share the same fate. In these cases, $z(L_-)$ is already fixed by the phase invariances of the two nontrivial components and an increase in $I(0)$ (and therefore $n(L_+)$) is not offset and will likely trigger an instability. We will examine this possibility in a later subsection.

3.4. Multi-component N-pulses, for $1/4 \leq r_i < r$. As seen in Jackson [3], the mechanism for N-pulse creation varies depending upon whether the bifurcation occurs when $r < 1/4$ or $r \geq 1/4$. Depending upon the nonlinearities $h_1(\cdot)$ and $h_2(\cdot)$, either case is possible.

Because any N-pulse is required to alternate in exactly one of its components between successive pulses, the N-pulse has $n(L_-) = iN + (N-1)$. Additionally, we still have $z(L_-) = 2$. We will now calculate $n(L_+)$ by carefully determining the winding number $I(0)$ along the pulse.

For each N, we find an N-pulse $U_N(x)$ by identifying an intersection of $(\Phi_{\text{far}} \circ \Phi_{\text{near}})^{(N)} \circ \Phi_{\text{far}} W_{\text{loc}}^{u}$ with the local stable manifold W_{loc}^{u}. In particular, we consider the manner in which the global unstable manifold W^u of the origin intersects consecutive sections Σ_{out} and Σ_{in} (and their reflections $S_1\Sigma_{\text{out}}$ and $S_1\Sigma_{\text{in}}$ defined near the origin, following successive excursions near the one-component pulse $(U_0(x), 0)$ (and its reflection $(-U_0(x), 0)$).

In order to compute $I(0)$, we initialize a vector $p(x)$, based at the point on the v_u-axis in Σ_{out} associated with the N-pulse, tangent to the v_u-axis so that W_{-}^{u} is spanned by the vector $U_N'(x)$ tangent to the pulse and $p(x)$. Evolving the 2-form $p(x) \wedge U_N'(x)$ via (9) between Σ_{out} and Σ_{in}, we note that when it reaches Σ_{in} this 2-form remains tangent to $\Phi_{\text{far}} W_{loc}^{u}$ and has undergone the same degree of winding as the 1-pulses in this regime. In particular, $\Phi_{\text{far}} W_{\text{loc}}^{u}$ connects the origin (representative of the single-component 1-pulse) and a point on the w_s-axis in Σ_{in} (this point represents the multi-component 1-pulse). The projection of $p(x)$ onto Σ_{in} continues to be tangent

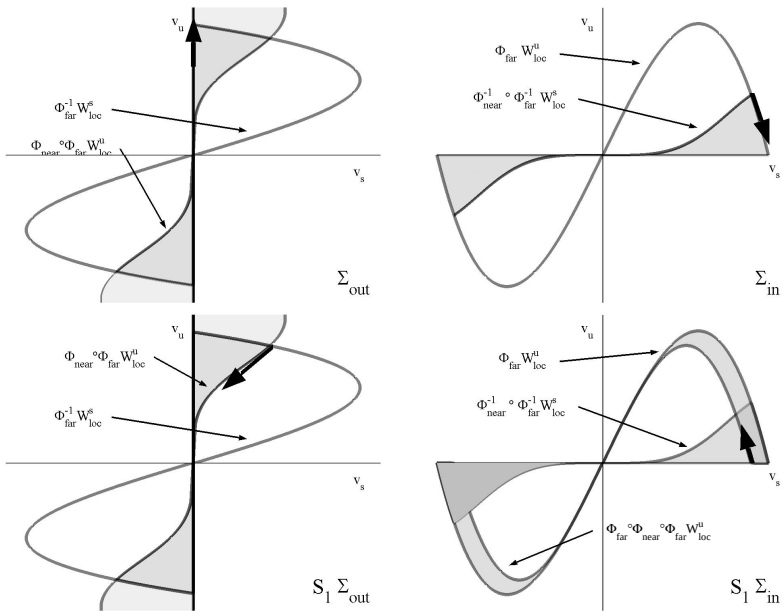

FIG. 5. *A view of the winding from the bifurcation picture for the N-pulse with bifurcation value $r_i \geq 1/4$. The orbit in $C(2)$ with α-limit $\tilde{W}^u_-$ gains $i+1$ winds with each excursion.*

to $\Phi_{\text{far}} W^u_{\text{loc}}$ and to point away from the origin.

However, as the single-component pulse is near degeneracy, the impending passage near the origin between the sections Σ_{in} and $S_1\Sigma_{\text{out}}$ may act to either increase the winding (as with the multi-component 1-pulse) or decrease the winding that has occured (as with the single-component 1-pulse) along the nearby N-pulse. This winding can again be determined by considering the bifurcation mechanism itself. For $r > 1/4$, curves approaching the origin transverse to the w_s-axis in Σ_{in} are taken far from the origin in $S_1\Sigma_{\text{out}}$. Similarly, a curve approaching any other point along the w_s-axis in Σ_{in} is taken to a curve tangent to the w_u-axis and approaching the origin in $S_1\Sigma_{\text{out}}$. In particular, the pertinent portion of the curve $\Phi_{\text{near}} \circ \Phi_{\text{far}} W^u_{\text{loc}}$ – the part containing the point corresponding to the N-pulse – approaches the origin tangent to the w_s-axis in $S_1\Sigma_{\text{out}}$ and the projection of $p(x)$ onto $S_1\Sigma_{\text{out}}$ is tangent to $\Phi_{\text{near}} \circ \Phi_{\text{far}} W^u_{\text{loc}}$ and now pointing *toward* the origin. As seen in Figure 5, the N-pulse therefore has winding of $i+2$ associated with this (and subsequently, each further) excursion along the pulse $\pm U_0(x)$ and hence

$$n(L_+) - z(L_-) - n(L_-) = N(i+2) - 2 - (iN + (N-1)) = N - 1 \ .$$

In this regime, then, the alternating N-pulses are necessarily unstable, with at least $N-1$ positive eigenvalues.

3.5. Multi-component N-pulses, for $r_i < r < 1/4$. The calculation in this regime begins in a similar manner, since we again have $n(L_-) = iN + (N-1)$ and $z(L_-) = 2$. It remains now to determine $n(L_+)$ by calculating the winding number $I(0)$ along the pulse.

As before, we follow successive iterates of the unstable manifold W^u of the origin along the N-pulse $U_N(x)$, and note the winding of the manifold spanned by $p(x) \wedge$

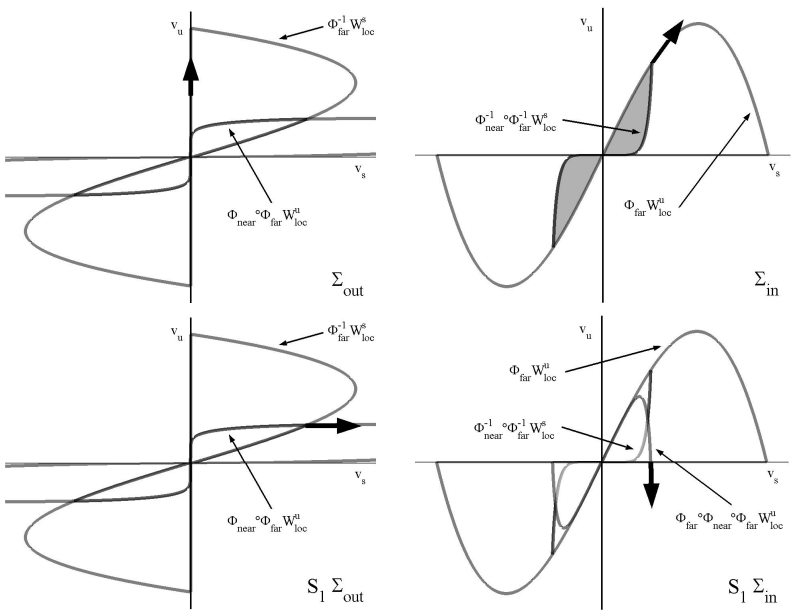

FIG. 6. *A view of the winding from the bifurcation picture for the N-pulse with bifurcation value $r_i < 1/4$. The orbit in $C(2)$ with α-limit $\hat{W}^u_-$ does not see as much winding in this regime, as the pass near the origin (the "glueing") does not reinforce the winding of the 1-pulse. The orbit gains only i winds with each excursion.*

$U'_N(x)$, where $p(x)$ is again initialized based at the point on the v_u-axis in Σ_{out} associated with the N-pulse, tangent to the v_u-axis.

Evolving the 2-form $p(x) \wedge U'_N(x)$ via (9) between Σ_{out} and Σ_{in}, this 2-form remains tangent to $\Phi_{\text{far}} W^u_{loc}$ when it reaches Σ_{in} and has undergone the same degree of winding as the 1-pulses in this regime. $\Phi_{\text{far}} W^u_{\text{loc}}$ connects the origin (representative of the single-component 1-pulse) and a point on the w_s-axis in Σ_{in} (representing the multi-component 1-pulse). The projection of $p(x)$ onto Σ_{in} continues to be tangent to $\Phi_{\text{far}} W^u_{\text{loc}}$ and to point away from the origin.

In this case, however, the passage near the origin between the sections Σ_{in} and $S_1\Sigma_{\text{out}}$ acts to decrease the winding. For $r < 1/4$, curves approaching the origin transverse to the w_s-axis in Σ_{in} are mapped to curves approaching the origin tangent to the w_u-axis; and a curve approaching any other point along the w_s-axis in Σ_{in} is taken to a curve tangent to the w_s-axis in $S_1\Sigma_{\text{out}}$. In particular, the pertinent portion of the curve $\Phi_{\text{near}} \circ \Phi_{\text{far}} W^u_{\text{loc}}$ approaches the origin tangent to the w_s-axis in $S_1\Sigma_{\text{out}}$ and the projection of $p(x)$ onto $S_1\Sigma_{\text{out}}$ is tangent to $\Phi_{\text{near}} \circ \Phi_{\text{far}} W^u_{\text{loc}}$ and continuing to point *away from* the origin. As seen in Figure 5, the N-pulse therefore only has winding $i+1$ associated with this (and all but the final) excursion along the pulse $\pm U_0(x)$. Since the final excursion ends with the the base point on the w_u-axis, and the global unstable manifold W^u transverse to it, the final excursion has winding $i+2$. See Figure 6. Therefore,

$$n(L_+) - z(L_-) - n(L_-) = [(N-1)(i+1) + (i+2)] - 2 - [iN + (N-1)] = 0 \ .$$

Amazingly, in this regime, then, the alternating N-pulses *are not necessarily unstable!!*

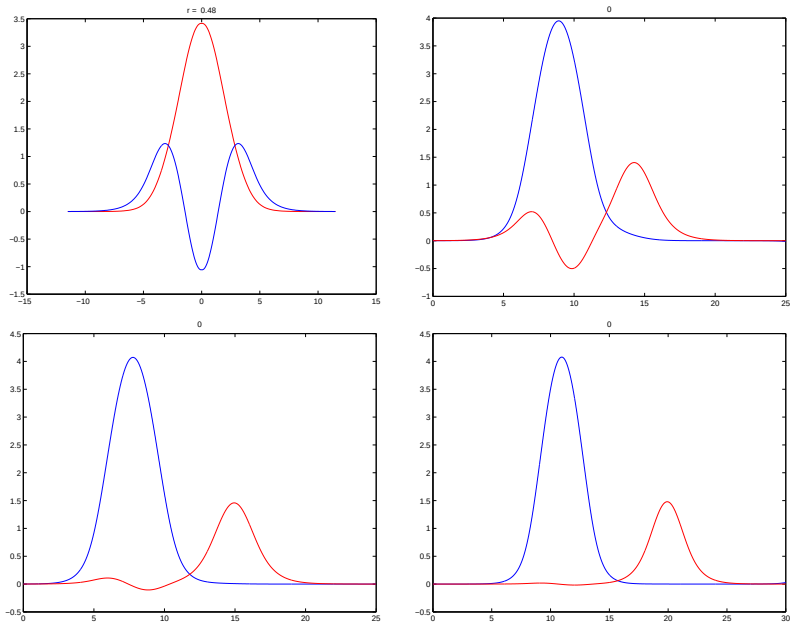

FIG. 7. *There are a pair of asymmetric multi-component pulses that bifurcate from the symmetric multi-component pulse when it becomes degenerate. Shown in this figure is the symmetric pulse when* $r = 0.48$ *and one of the bifurcating pulses for* $r = 0.50$, $r = 0.52$ *and* $r = 0.5275$. *(The other is simply its reflection in the vertical plane.)*

3.6. A secondary bifurcation of asymmetric pulses. It is straightforward to use the expression for κ given in (3.2) to numerically calculate $I(0)$, and hence $n(L_+)$ for the 1-pulses seen so far. We note especially that $I(0)$ may increase as we follow the multi-component 1-pulse away from the initial bifurcation. Beyond such a point, the multi-component 1-pulse will be inherently unstable, with at least one positive eigenvalue.

However, the change in $I(0)$ signals the passage through degeneracy of the multi-component 1-pulse, and we expect a further bifurcation of pulses at this point. In this case, since the multi-component 1-pulse is not in orbit-flip configuration, we do not expect a cascade of N-pulses. The results of Knobloch [12] apply in this case and we see a pair of asymmetric pulses bifurcating from the (symmetric) multi-component 1-pulse. Such bifurcating pulses are shown in Figure 7.

Additionally, these new asymmetric multi-component 1-pulses inherit the winding number of the symmetric multi-component 1-pulse from before the bifurcation, and hence these pulses *may, in fact, be stable!* The winding numbers for the symmetric multi-component 1-pulse and the asymmetric pulses bifurcating from it are shown in Figure 8.

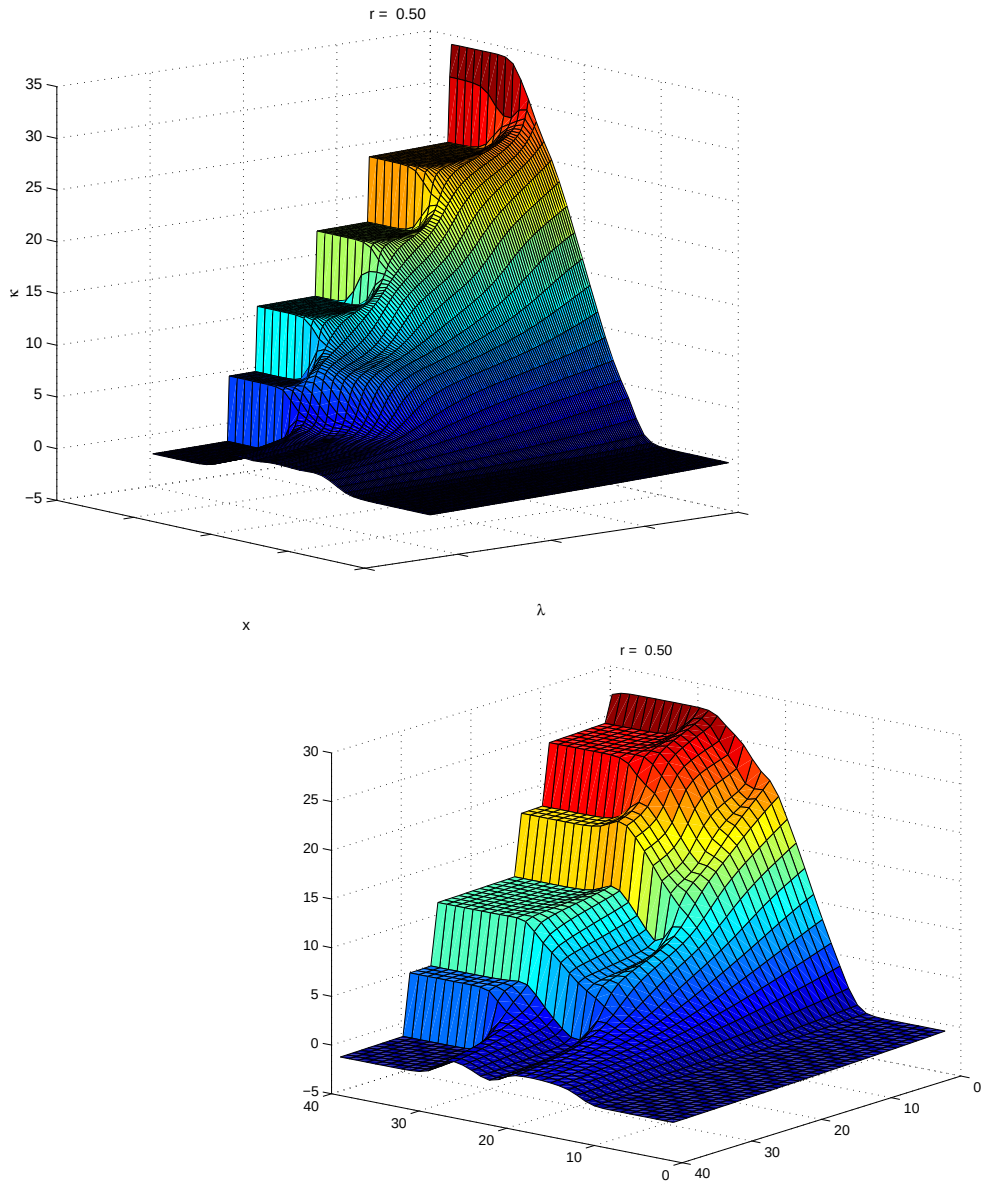

FIG. 8. *Numerical computation of $n(L_+)$ for the multi-component 1-pulse (above,left) and the asymmetric multi-component 1-pulse bifurcating from it (below,right), at $r = 0.50$, after the symmetric pulse has passed through degeneracy. The angular variable $\kappa(x)$ is shown for increasing values of the eigenvalue parameter λ. λ values for which λ is an eigenvalue are seen as steps – for λ values on either side of these steps, the orbit in $C(2)$ goes to different components of the train. The highest "half–step" is associated with the eigenvalue $\lambda = 0$. For the symmetric pulse, a new eigenvalue has appeared with λ small. Now $I(0) = 6$, and hence $n(L_+) - z(L_-) - n(L_-) = 5-2-2 = 1$ and the multi-component 1-pulse is necessarily unstable in this regime. For the asymmetric pulse, we still have $I(0) = 5$, and hence $n(L_+) - z(L_-) - n(L_-) = 4 - 2 - 2 = 0$. The asymmetric bifurcating pulses may indeed be stable!*

REFERENCES

[1] M. Haelterman and A. Sheppard, *Bifurcation phenomena and multiple soliton–bound states in isotropic Kerr media,* Phys. Rev. E **49** (1994), 3376–3381.

[2] E. A. Ostrovskaya and Y. S. Kivshar, *Multihump optical solitons in a saturable medium,* J. Opt. B **1** (1999), 77–83.

[3] R.K. Jackson, *A homoclinic flip bifurcation in nonlinearly coupled Schrödinger equations.* Submitted.

[4] E. A. Ostrovskaya, Y. S. Kivshar, D. V. Scryabin and W. J. Firth, *Stability of multihump optical solitons,* Phys. Rev. Lett. **83** (1999), 296–299.

[5] D. Henry, *Geometric theory of semilinear parabolic equations*, Lecture Notes in Math., 840, Springer, Berlin, 1981.

[6] T. Kapitula and B. Sandstede, *Stability of bright solitary–wave solutions to perturbed nonlinear Schrödinger equations,* Physica D **124** (1998), 58–103.

[7] D. E. Pelinovsky and J. Yang, *Instabilities of multi-hump vector solitons in coupled nonlinear Schrödinger equations.* Submitted.

[8] C. K. R. T. Jones, *Instability of standing waves for non–linear Schrödinger–type equations,* Ergodic Theory Dynam. Systems **8** (1988), 119–138.

[9] M. Grillakis, *Analysis of the linearization around a critical point of an infinite-dimensional Hamiltonian system,* Comm. Pure Appl. Math. **43** (1990), 299–333.

[10] A. C. Yew, *An analytical study of solitary–waves in quadratic media*, PhD thesis, Brown University, (1998).

[11] J. Deng, *Instability of waves and patterns in Hamiltonian systems and the Maslov index*, PhD thesis, Brown University, (2002).

[12] J. Knobloch, *Bifurcation of degenerate homoclinic orbits in reversible and conservative systems,* J. Dynam. Differential Equations **9** (1997), 427–444.

[13] S. Nii, *N–homoclinic bifurcations for homoclinic orbits changing their twisting,* J. Dynam. Differential Equations **8** (1996), 549–572.

[14] V. I. Arnol'd, *On a characteristic class entering into conditions of quantization. (Russian),* Funkcional. Anal. i Priložen. **1** (1967), 1–14.

[15] A. Bose and C. K. R. T. Jones, *Stability of the in-phase travelling wave solution in a pair of coupled nerve fibers,* Indiana Univ. Math. J. **44** (1995), 189–220.

[16] R. K. Jackson and M. I. Weinstein, *Geometric analysis of bifurcation and symmetry breaking in a Gross-Pitaevskii equation,* J. Statist. Phys. **116** (2004), 881–905.